

Variable-Temperature Rate Coefficients of Proton-Transfer Equilibrium Reaction $C_2H_4 + H_3O^+ \rightleftharpoons C_2H_5^+ + H_2O$ Measured with a Coaxial Molecular Beam Radio Frequency Ring Electrode Ion Trap

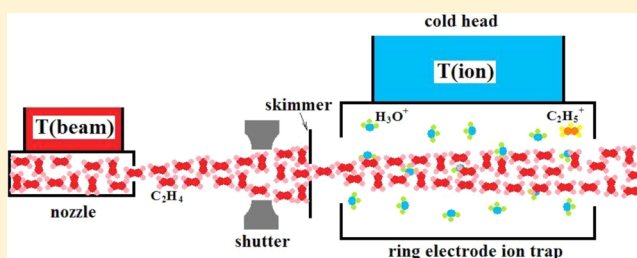
Mark A. Smith,^{*,†,‡,§} Bing Yuan,[†] and Andrei Sanov[†]

[†]Department of Chemistry and Biochemistry, University of Arizona, 1306 East University Boulevard, Tucson, Arizona 85721, United States

[‡]Department of Planetary Science, Lunar and Planetary Laboratory, University of Arizona, 1629 East University Boulevard, Tucson, Arizona 85721, United States

[§]Department of Chemistry, University of Houston, Houston, Texas 77204, United States

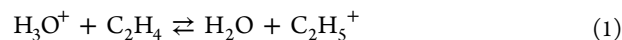
ABSTRACT: The rate coefficients for the forward and reverse proton-transfer reactions $C_2H_4 + H_3O^+ \rightleftharpoons C_2H_5^+ + H_2O$ are studied with respect to independent varied neutral molecule and ion temperatures. The measurements are performed using a coaxial molecular beam radio frequency ring electrode ion trap at trap temperatures down to 23 K and beam temperatures up to 450 K. The temperature-dependent rate coefficients suggest that in this temperature window, the reaction proceeds through a statistically equilibrated complex. In order to explain the observed rate coefficients, a new type of reaction temperature was defined in these studies that considered collisional and internal (rotational and vibrational) degrees of freedom of both H_3O^+ and C_2H_4 . The enthalpy and entropy of the equilibrium reaction deduced from a Van't Hoff plot are $\Delta H = (5.1 \pm 0.5) \text{ kJ}\cdot\text{mol}^{-1}$ and $\Delta S = (-15.0 \pm 0.9) \text{ J}\cdot\text{mol}^{-1}\cdot\text{K}^{-1}$, respectively.



INTRODUCTION

Proton-transfer reactions of simple molecules play significant roles in dense interstellar clouds as they can effectively produce neutral molecules.¹ Rate coefficient determination for proton transfer is important in modeling complex chemistry in the interstellar medium (ISM) and the studies of the relative proton affinity between different acids.² H_3O^+ , H_2O , C_2H_4 , and $C_2H_5^+$ are all detected in the ISM and are essential intermediates in the production of complicated oxygenated organic molecules.

The endothermic proton-transfer equilibrium reaction



has been well studied in the past.^{3–6} In the present study, a coaxial molecular beam radio frequency ring electrode trap (CoMB-RET) is applied to measure the forward and reverse rate coefficients of this reaction, with molecular beam and ion temperatures varied independently from 300 to 450 K and from 25 to 350 K, respectively. From these data, the thermodynamics of equilibrium 1 in the low temperature window are determined and compared to past studies.

The results also have significant implications to the reaction mechanism at low collision temperatures. There are two common types of reaction mechanisms in gas-phase ion–molecule reactions: direct collision through stripping dynamics at high collision energy (more than several electron-volts) and complex-mediated reaction through long-range attraction when

the collision energy is lower than 1 eV.^{7,8} The results of the present study strongly support a long-lived complex mechanism, where all degrees of freedom (DOFs) in both reactants participate equally as energy baths in driving the endothermic proton transfer from H_3O^+ to the ethylene molecule.

EXPERIMENTAL SECTION

A CoMB-RET instrument that has been specifically designed to minimize trap interactions with ion source gas or background beam molecule contamination is used in this study. The trap in the current configuration is a ring electrode trap that has been previously described in the literature.^{9,10}

The reactant ions H_3O^+ of the forward reaction are produced by electron impact in a U-shaped radio frequency trap with a H_2O vapor pressure of approximately 5×10^{-5} Torr. Reactant ions $C_2H_5^+$ for the reverse reaction are produced in the ion source area from collisions between $C_2H_4^+$ ions that are formed by electron impact and C_2H_4 neutral molecules with a C_2H_4 vapor pressure of approximately 1×10^{-4} Torr. These conditions maximize the $C_2H_5^+$ exiting the trap from this reactive environment (with ion cooling reserved for the RET stage). Trajectories of the ions exiting the ion source are bent 90° by a dc quadrupole bender, which separates the ion stream

Received: June 28, 2012

Revised: November 9, 2012

Published: November 12, 2012

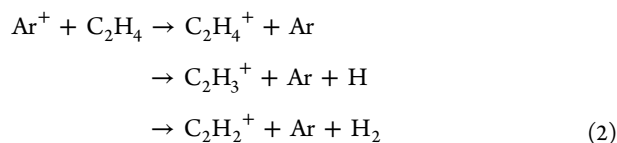
from the effusive gas exiting the source. The ions are then focused into a double-quadrupole ion guide/mass selector. The mass-selected ion beam is then turned another 90°, bringing it to a coaxial alignment with both the RET axis and the molecular beam.

Ions at low energy (<0.1 eV) are injected into the RET, which is mounted on the end of a thermally regulated liquid He cryostat (Janis Model ST-400), used to vary the trap temperature between 20 and 450 K. Buffer gas admitted to the trap equilibrates to the defined wall temperature, as do the ions through buffer gas collisions. Buffer cooling is used to equilibrate the stored ions with the thermal conditions of the trap walls. After ions are cooled and most of the He buffer is pumped out of the RET, the stored ions react with a chopped neutral molecular beam for several hundred milliseconds to a few seconds (usually <5 s). Following the reaction period, the remaining reactant and newly created product ions are allowed to enter the quadrupole analyzer, where they are accelerated, mass-selectively filtered, and detected using a fast microchannel plate (MCP) ion counting system.

The molecular beam nozzle consists of a 50 mm long, 0.5 mm internal diameter tube mounted onto the end of a second thermally regulated cryostat. For the forward reaction, the stagnation pressure of C₂H₄ is (65 ± 1) Torr, while in the reverse reaction, the stagnation pressure of H₂O is (20 ± 1) Torr. The beam passes through a 0.5 mm orifice conical skimmer (Beam Dynamics, Inc.) mounted 20 mm downstream and is then skimmed a second time, 300 mm downstream from the nozzle, using a 2 mm diameter flat aperture, and it becomes coaxial with the trap. A regulated shutter is placed in the beam path in front of the second skimmer. The shutter is opened after the stored ions in the RET have been cooled and is kept open for a desired time depending on the reaction period in the trap. The molecular beam terminates in the chamber of a residual gas analyzer (RGA; Stanford Research Systems 200), which is used to calibrate the number density of the molecular beam.

RESULTS AND DISCUSSION

(1). Beam Number Density Calibration. In order to determine the ethylene beam number density in the RET, the reaction Ar⁺ + C₂H₄ with a known rate coefficient ($k_2 = 1.10 \times 10^{-9} \text{ cm}^3 \cdot \text{s}^{-1}$ at 300 K¹¹) is used.



Product ions C₂H₂⁺, C₂H₃⁺, and C₂H₄⁺ are all observed at the detector, and secondary product ions C₂H₅⁺ and C₃H₅⁺ created from collisions between initial product ions C₂H₂⁺, C₂H₃⁺, and neutral molecule C₂H₄^{11–13} are also detected. The growth of the sum of all of the observed product ions as well as the loss of Ar⁺ ions is used to get a self-consistent determination of the ethylene beam number density.

The number density of ethylene in the RET is calibrated to be $2.5 \times 10^9 \text{ cm}^{-3}$ at 300 K and is inversely proportional to the square root of the beam temperature.

Molecular dimers are easily formed at low molecular beam temperatures (<220 K);¹⁰ however, at 300 K and higher beam temperatures, the ethylene dimer fraction in the beam is less than 0.01%, and the effect of dimers on the calibration reaction

and subsequent proton-transfer equilibrium studies is insignificant.

The calibration of the H₂O molecular beam has been described in our previous study.¹⁴ The temperature of the H₂O beam is varied from 300 to 400 K, and the product between the ions and H₂O clusters is not observed in the system. The number density of the H₂O beam at 300 K in the reaction system is $7.5 \times 10^7 \text{ cm}^{-3}$. No evidence of water dimers is observed with an absence of both H₃O⁺ and multioxygenated ions in the beam monitor.

(2). Measurement of the Forward Rate Coefficient, H₃O⁺ + C₂H₄. The rate coefficient of the forward reaction H₃O⁺ + C₂H₄ was measured at different beam and trap temperatures. Besides the primary product ions, C₂H₅⁺, secondary C₃H₅⁺ formed by collisions between C₂H₅⁺ and C₂H₄ neutral molecules are also observed in the system. The ion fraction of all of the reactant and product ions as a function of trapping time at a trap temperature of 80 K and a beam temperature of 300 K are shown in Figure 1. Because the

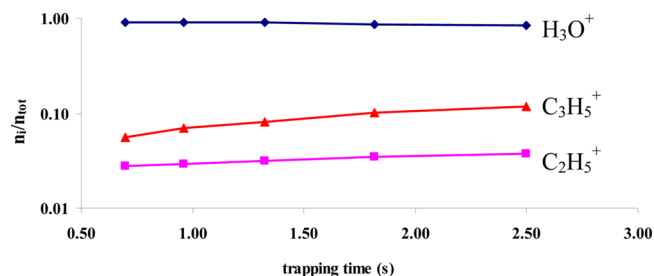


Figure 1. The relative temporal concentration of H₃O⁺, C₂H₅⁺, and C₃H₅⁺ ions in the RET for the reaction of H₃O⁺ and C₂H₄. The number density of the C₂H₄ beam is $2.5 \times 10^9 \text{ molecule} \cdot \text{cm}^{-3}$. As discussed in the text, the C₃H₅⁺ is a secondary product of the reaction of C₂H₅⁺ and C₂H₄.

reaction between C₂H₅⁺ and C₂H₄ producing C₃H₅⁺ is a fast reaction at near the capture rate, a great percentage of C₂H₅⁺ ions are consumed. When the rate coefficients of the forward reaction H₃O⁺ + C₂H₄ are calculated, both C₂H₅⁺ and C₃H₅⁺ are counted as the proton-transfer product C₂H₅⁺ as C₃H₅⁺ is created from C₂H₅⁺. Figure 2 shows the observed rate coefficients of proton-transfer reaction H₃O⁺ + C₂H₄ at different collision temperatures. The center of mass collision temperature is defined as

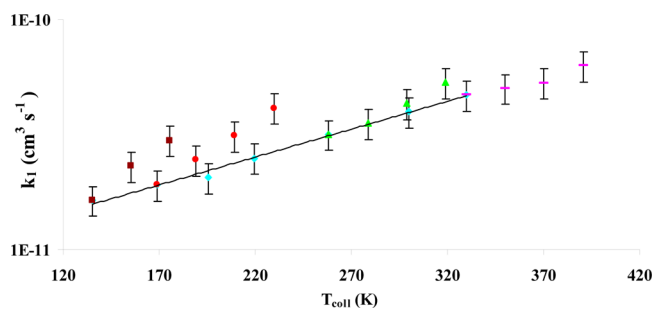


Figure 2. Rate coefficients $k_1(T_{\text{coll}})$ observed with varying beam, T_{beam} , and trap, T_{trap} , temperatures. For variation of T_{beam} from 300 to 450 K, data were obtained for trap temperatures of 23 (purple ■), 80 (red ●), 230 (green ▲), and 350 K (□ pink bars). For variation of T_{trap} from 23 to 350 K, data were obtained for a beam temperature of 300 K (cyan ◆) with this single series of data fit to a straight line.

$$T_{\text{coll}} = \frac{m_{\text{ion}} T_{\text{beam}} + m_{\text{beam}} T_{\text{ion}}}{m_{\text{ion}} + m_{\text{beam}}} \quad (3)$$

where m_{ion} is the mass of H_3O^+ , T_{ion} is the trap temperature, m_{beam} is the mass of C_2H_4 , and T_{beam} is the beam temperature, which under effusive conditions is equal to the nozzle temperature. As shown in Figure 2, by varying the trap and beam temperatures independently, rate coefficients can be determined at equivalent collision temperatures but different degrees of excitation of the ion and neutral molecule degrees of freedoms (DOFs). At a beam temperature of 300 K, the rate coefficients at different trap temperatures define a smooth monotonic function; however, the rate coefficients have a quite different beam temperature dependence at fixed trap temperatures.

Therefore, the collision temperature alone does not account for the energy brought to bear on the endothermic barrier by the two reactants with different internal DOFs. A new temperature should be defined for the reaction system to account statistically for the internal and external energies contributed in a collision. We assume complete equilibration of internal and external DOFs for each specific reactant, which implies that all ion motions are described by the trap wall temperature, while the nozzle temperature completely describes the motion of the neutrals in the effusive beam (no expansive cooling). For the 10 atom collision system, $\text{H}_3\text{O}^+ + \text{C}_2\text{H}_4$, there are 27 DOFs in the center of mass frame. There are three center of mass translational DOFs whose energy moments are given by T_{coll} in eq 3. The H_3O^+ ion has 9 internal DOFs (3 rotational, 6 vibrational), while C_2H_4 has 3 rotational and 12 vibrational DOFs. Independent of energy spacing, each DOF brings an average of $(1/2)kT_i$ to the collision over the ensemble average appropriate to a rate coefficient measurement. Here, T_i is the temperature appropriately describing the energy distribution of the specific DOF.

In this case, we can define a reaction temperature, T_{react} , describing the total internal energy moment of the $\text{H}_3\text{O}^+ \cdot \text{C}_2\text{H}_4$ collision pair.

$$T_{\text{react}} = \left(\frac{3}{27}\right)T_{\text{coll}} + \left(\frac{9}{27}\right)T_{\text{trap}} + \left(\frac{15}{27}\right)T_{\text{beam}} \quad (4)$$

where T_{coll} is the collision temperature defined in eq 3. The second and third terms in eq 4 represent the internal temperature contribution of the H_3O^+ ions and C_2H_4 , respectively.

If we compare rate coefficients for reaction 1 against T_{react} we obtain the relationship shown in Figure 3. Here, we see that independent of the energy source, be it collisional, internal to the ion, or internal to the neutral, we find a common relationship within experimental error. This strongly suggests complete equilibration of energy in the $\text{H}_3\text{O}^+ \cdot \text{C}_2\text{H}_4$ collision complex as the system surmounts the endothermic barrier.

Comparison of this rate coefficient data for the forward reaction with the previous measurements from McIntosh and Bohme is shown in Figure 4. It is found that the rate coefficient has steeper temperature dependence in McIntosh's result than that in this study but is mainly influenced by the low-temperature measurement near 200 K. In the measurement from McIntosh, a selected ion flow tube (SIFT) was used with a background He pressure of 0.45 Torr. In this case, the rate of the three-body association reaction

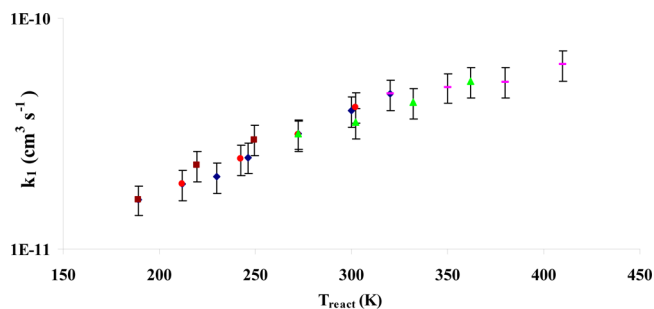
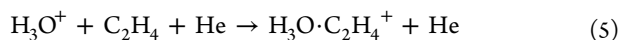


Figure 3. Temperature-dependent rate coefficients, $k_1(T_{\text{react}})$, of the forward proton-transfer reaction $\text{H}_3\text{O}^+ + \text{C}_2\text{H}_4$ plotted against T_{react} defined in eq 4. For variation of T_{beam} from 300 to 450 K, data were obtained for trap temperatures of 23 (purple ■), 80 (red ●), 230 (green ▲), and 350 K (□ pink bars). For variation of T_{trap} from 23 to 350 K, data were obtained for a beam temperature of 300 K (blue ◆).

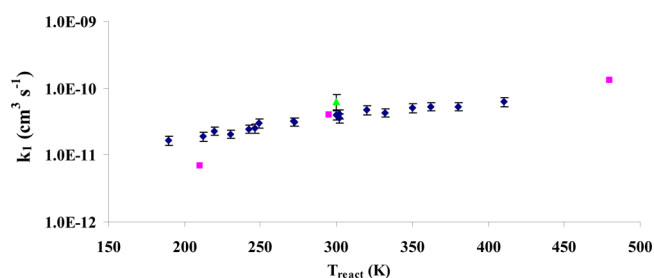


Figure 4. Comparison of the rate coefficients, $k_1(T_{\text{react}})$, of the forward reaction $\text{H}_3\text{O}^+ + \text{C}_2\text{H}_4$: (blue ◆) this study, (pink ■) McIntosh et al. (ref 6), and (green ▲) Bohme et al. (ref 5).

is comparable with the rate of the forward reaction,⁶ and it becomes faster at lower reaction temperature. In McIntosh's study, at 210 K, there is a 90% three-body association reaction in the system; at 295 K, it is 60%, and at 480 K, it is 0%. The percentage difference of three-body association reaction 5 at different reaction temperatures might cause a problem in the rate coefficient deviation of the forward reaction, which makes the rate coefficient have a steeper temperature dependence. In our study, the background pressure in the RET is 2×10^{-8} Torr; thus, no three-body association product is observed in our system.

(3). Measurement of the Reverse Reaction, $\text{C}_2\text{H}_5^+ + \text{H}_2\text{O}$. The reverse reaction in the equilibrium reaction 1 is a fast exothermic proton transfer whose rate coefficient was measured at several reaction temperatures. In this context, the appropriate reaction temperature for k_{-1} is given by

$$T_{\text{react}}(k_{-1}) = \left(\frac{3}{27}\right)T_{\text{coll}} + \left(\frac{6}{27}\right)T_{\text{beam}} + \left(\frac{18}{27}\right)T_{\text{trap}} \quad (6)$$

This new data is shown in Figure 5, together with the data from the previous study by McIntosh and co-workers.⁶ The combined data set is found to be very well fit by a common relationship (using appropriate temperatures for the independent studies) given by

$$k_{-1}(\text{cm}^3 \text{s}^{-1}) = 2.55 \times 10^{-9} - 2.69 \times 10^{-12}T \quad (7)$$

which is slightly inversely temperature-dependent, consistent with the polarity of H_2O . We can use this fit to the experimental data for k_{-1} , given in eq 7, to determine the equilibrium constant $K_{\text{eq}}(T_{\text{react}})$ for each temperature, T_{react} for which k_1 was measured. The relationship between $K_{\text{eq}}(T_{\text{react}})$

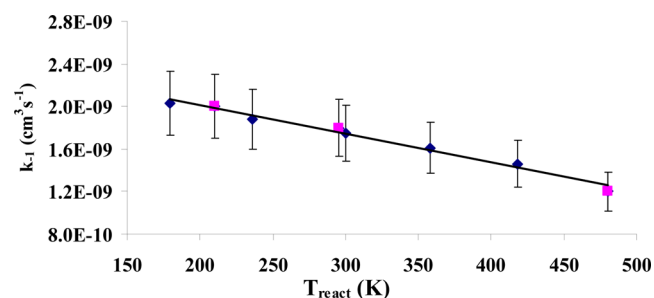


Figure 5. Comparison of rate coefficients, $k_{-1}(T_{\text{react}})$, of the reverse reaction $\text{C}_2\text{H}_5^+ + \text{H}_2\text{O}$: (blue \blacklozenge) this study and (pink \blacksquare) McIntosh et al. (ref 6).

and $1/T_{\text{react}}$ in a typical Van't Hoff relationship, allows determination of the enthalpy, ΔH_r° , entropy, ΔS_r° , and ΔG° for reaction 1, as shown in Figure 6. From the slope and

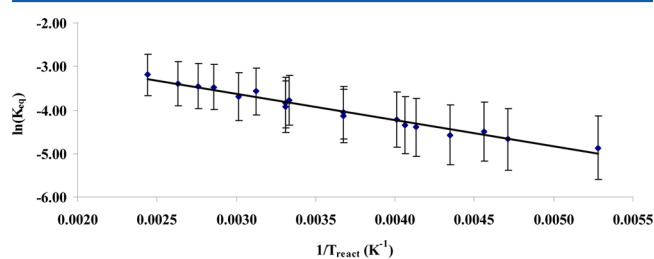


Figure 6. Van't Hoff plot of $K_{\text{eq}}(T_{\text{react}})$ versus $1/T_{\text{react}}$ for the equilibrium reaction 1.

intercept of the relationship, we determine in the temperature window of 180–450 K that $\Delta H = (5.1 \pm 0.5) \text{ kJ}\cdot\text{mol}^{-1}$ and $\Delta S = (-15.0 \pm 0.9) \text{ J}\cdot\text{mol}^{-1}\cdot\text{K}^{-1}$. The values determined in this work compare favorably with past determinations, as shown in Table 1. Our ΔH data are in close agreement with the value

Table 1. Comparison of the Experimental Enthalpy ΔH , Entropy ΔS , and Standard Free Energy ΔG at 300 K for the Equilibrium Reaction $\text{C}_2\text{H}_4 + \text{H}_3\text{O}^+ \rightleftharpoons \text{C}_2\text{H}_5^+ + \text{H}_2\text{O}$ between This Work and Previous Studies

	ΔH ($\text{kJ}\cdot\text{mol}^{-1}$)	ΔS ($\text{J}\cdot\text{mol}^{-1}\cdot\text{K}^{-1}$)	$\Delta G_{300\text{K}}$ ($\text{kJ}\cdot\text{mol}^{-1}$)
Bohme, D. K. ^a	5.8 ± 5.0	-9.6 ± 18.8	7.5 ± 0.8
McIntosh, B. J. ^b	10.4	4.2	9.6
Collyer, S. M. ^c	17.1	9.2	14.2
McMahon, T. B. ^d	15.9 ± 2.1	5.0 ± 4.2	14.4 ± 0.8
our work	5.1 ± 0.5	-15.0 ± 0.9	9.6 ± 0.8

^aReference 5. ^bReference 6. ^cReference 4. ^dReference 3. In ref 3, ΔH and ΔS are given at 400 K and are used without correction to calculate $\Delta G_{300\text{K}}$.

provided by Bohme, which equals $(5.8 \pm 5.0) \text{ kJ}\cdot\text{mol}^{-1}$, and the difference between the two ΔG values is $2.1 \text{ kJ}\cdot\text{mol}^{-1}$, just outside of the estimated errors. Bohme measured the rate coefficients of reaction 1 only at 300 K, and the ΔS that they used is estimated from theoretical calculation, which might cause a problem in the determination of ΔG . The ΔG value provided by McIntosh is the same as ours, but the ΔH and ΔS values are quite different. The steeper temperature dependence of the rate coefficients for the forward reaction in their measurement gives higher ΔH and ΔS values, compared to our result. The reason for the discrepancy is discussed above, in

the second part of the discussion. ΔG values provided by Collyer and McMahon, which are calculated from the measurements of several equilibrium reactions, are about $6 \text{ kJ}\cdot\text{mol}^{-1}$ higher than those in this study. As these values are not deduced from direct measurements, errors should be accumulated through the combination of experimental results. It is not surprising that these values are outside of the error window of the direct measurements. The present work significantly constrains the determination of this reaction thermochemistry and has significantly reduced the error and better defined the optimal values to be employed in future modeling of environments incorporating this reaction.

CONCLUSION

Using a coaxial molecular beam ring electrode trap reaction method, the proton-transfer equilibrium reaction $\text{C}_2\text{H}_4 + \text{H}_3\text{O}^+ \rightleftharpoons \text{C}_2\text{H}_5^+ + \text{H}_2\text{O}$ was studied. The temperatures of both the molecular beam and ion trap were controlled independently, and the reaction temperature was defined as a degree-of-freedom-weighted average of the energy modes brought to the reaction complex. It is verified that the forward proton-transfer reaction $\text{H}_3\text{O}^+ + \text{C}_2\text{H}_4$ behaves statistically as all available energy is equally available and therefore randomized within the reaction complex as it surmounts the barrier. The enthalpy ΔH_r° and entropy ΔS_r° of the equilibrium reaction 1 are calculated to be $\Delta H_r^\circ = (5.1 \pm 0.5) \text{ kJ}\cdot\text{mol}^{-1}$ and $\Delta S_r^\circ = (-15.0 \pm 0.9) \text{ J}\cdot\text{mol}^{-1}\cdot\text{K}^{-1}$, respectively. Besides being in reasonable agreement with previous studies, these values are better defined with higher accuracy and precision through this investigation.

AUTHOR INFORMATION

Corresponding Author

*Address: Smith College of Natural Sciences and Mathematics, University of Houston, 214 Science & Research Bldg 1, Houston, TX 77204-5008, U.S.A. Phone: 713/743-3755. Fax: 713/743-8630. E-mail: markasmith@nsm.uh.edu.

Notes

The authors declare no competing financial interest.

ACKNOWLEDGMENTS

We would like to acknowledge the National Science Foundation for partial support of this work through Awards CHE-0618735 and CHE-0513364 and the Office of the Vice President for Research, University of Arizona for their contributing support. In addition, we must thank Dr. Dieter Gerlich, Dr. George Tikhonov, and Zachary Scott for their assistance in instrument design and construction. We would like to thank Dr. Darin Latimer and Sciex for their assistance with the development of the quadrupole filters. We would also like to thank Prof. Bonner Denton and Paul Wentholt for assistance with this development effort.

REFERENCES

- (1) Smith, D. *Chem. Rev.* **1992**, *92*, 1473–1485.
- (2) Spanel, P.; Smith, D. *Int. J. Mass Spectrom.* **1998**, *181*, 1–10.
- (3) McMahon, T. B.; Kebarle, P. *J. Am. Chem. Soc.* **1985**, *107*, 2612–2617.
- (4) Collyer, S. M.; McMahon, T. B. *J. Phys. Chem.* **1983**, *87*, 909–911.
- (5) Bohme, D. K.; Mackay, G. I. *J. Am. Chem. Soc.* **1981**, *103*, 2173–2175.

- (6) McIntosh, B. J.; Adams, N. G.; Smith, D. *Chem. Phys. Lett.* **1988**, *148*, 142–148.
- (7) Levandier, D. J.; Varley, D. F.; Farrar, J. M. *J. Chem. Phys.* **1992**, *97*, 4008–4017.
- (8) Palm, H.; Alcaraz, C.; Millie, P.; Dutuit, O. *Int. J. Mass Spectrom.* **2006**, *249–250*, 31–44.
- (9) Gerlich, D. Inhomogeneous RF Fields: A Versatile Tool for the Study of Processes with Slow Ions. In *Stated-Selected and State-to-State Ion-Molecular Reaction Dynamics. Part 1. Experimental*; Ng, C. Y., Baer, M., Eds.; Advances in Chemical Physics Series; Wiley: New York, 1992; Vol. *LXXXII*.
- (10) Smith, M. A.; Yuan, B.; Sanov, A. *J. Phys. Chem. A* **2012**, DOI: 10.1021/jp305936f.
- (11) Tsuji, M.; Kouno, H.; Matsumura, K.; Funatsu, T.; Nishimura, Y.; Obase, H.; Kugishima, H.; Yoshida, K. *J. Chem. Phys.* **1993**, *98*, 2011–2022.
- (12) Hawley, M.; Mazely, T. L.; Randeniya, L. K.; Smith, R. S.; Zeng, X. K.; Smith, M. A. *Int. J. Mass Spectrom. Ion Processes* **1990**, *97*, 55–86.
- (13) McEwan, M. J.; Scott, G. B. I.; Anicich, V. G. *Int. J. Mass Spectrom. Ion Processes* **1998**, *172*, 209–219.
- (14) Yuan, B.; Scott, Z.; Tikhonov, G.; Gerlich, D.; Smith, M. J. *Chem. Phys.* **2011**, *115*, 25–29.